Wave Motion 48 (2011) 515–524

Contents lists available at ScienceDirect

Wave Motion

journal homepage: www.elsevier.com/locate/wavemoti

Exterior cloaking with active sources in two dimensional acoustics

Fernando Guevara Vasquez *, Graeme W. Milton, Daniel Onofrei

Mathematics Department, University of Utah, 155 S 1400 E RM 233, Salt Lake City UT 84112, USA

ARTICLE INFO

Article history:
Received 10 September 2010
Received in revised form 17 March 2011
Accepted 31 March 2011
Available online 8 April 2011

Keywords:
Active cloaking
Acoustic waves
Helmholtz equation
Green's formula

ABSTRACT

We cloak a region from a known incident wave by surrounding the region with three or more devices that cancel out the field in the cloaked region without significantly radiating waves. Since very little waves reach scatterers within the cloaked region, the scattered field is small and the scatterers are for all practical purposes undetectable. The devices are multipolar point sources that can be determined from Green's formula and an addition theorem for Hankel functions. The cloaking devices are exterior to the cloaked region.

1. Introduction

Interest in cloaking has surged, as reflected in the many recent reviews [2,3,10]. We introduced a new kind of cloaking for the two-dimensional Helmholtz equation [11,12]. Our approach uses *active sources* (cloaking devices) to hide objects placed in an external region. The advantages of our approach are: (a) by the superposition principle a cloak can be designed for a broad band of frequencies (excluding discretely many frequencies where the object being cloaked, if non-absorbing, "resonates") and (b) the cloak does not need materials with extreme properties which are hard to realize and dispersive, as it is the case in most transformation based cloaking strategies (see e.g. [6,8,10,16,23] — though an exception is [17]). A significant drawback of our approach is that we assume full knowledge of the incident field. Also the active sources contain a monopole term which may be problematic for applications in electromagnetism.

The problem of finding source distributions for cloaking is clearly ill-posed in the sense that if it admits one solution then it admits infinitely many solutions. In [11,12] we computed particular solutions involving three point-like devices by solving a constrained least-squares problem with the singular value decomposition (SVD). In an effort to explain rigorously our previous results, we use the Green representation theorem for the Helmholtz equation (in short *Green's formula*, see e.g. [5]), to derive explicitly a particular solution in terms of the incident field (Theorem 1).

Another cloaking method based on Green's formula is the active interior cloak introduced by Miller [19], which uses single and double layer potentials to cancel the incident field inside a closed curve. Cancelling fields inside (or outside) a region surrounded by active sources is known in acoustics as "active sound control" and has applications to e.g. noise suppression. We point to the reviews on active sound control by Peterson and Tsynkov [24] and Ffowcs Williams [7] and to the early work by Malyuzhinets [18]. Jessel and Mangiante [13] recognized that the single and double layer potentials from Green's formula can be hard to realize and showed that they can be replaced by a source density in an annular region containing the curve. Here we apply an addition theorem for Hankel functions to replace the source distribution on a curve by a few active sources, effectively connecting the cloaked region with the exterior. The sources we get are, as the ansatz used in [11,12], multipolar point-like sources: they are given as a series of cylindrical radiating solutions to the Helmholtz equation, centered at a few points. We also establish convergence of the series to the fields required for cloaking and give a specific configuration of sources (Section 2.3) similar to the one we found empirically in [11,12]. The

* Corresponding author.
E-mail addresses: fguevara@math.utah.edu (F. Guevara Vasquez), milton@math.utah.edu (G.W. Milton), onofrei@math.utah.edu (D. Onofrei).

0165-2125/$ – see front matter © 2011 Elsevier B.V. All rights reserved.
doi:10.1016/j.wavemoti.2011.03.005

problem of controlling the sources in the time domain so that the desired cloaking effect is achieved is not considered here and is left for future studies.

Other methods for obtaining exterior cloaks include those based on complementary media [14], surface plasmonic resonances [25], anomalous resonances in the vicinity of a superlens [20–22] and waveguides [26].

A different idea is that of illusion optics [15] where the goal is to hide an object and make it appear as another object. The Green's formula based approach that we present here also explains why this can be done using active devices, as was recently observed numerically [27]. We give a way of explicitly constructing the devices to such effect, without the need for solving a least-squares problem (see Remark 4).

We work in the frequency domain at a fixed angular frequency ω. In a medium with constant speed of propagation c, the wave field $u(\mathbf{x},\omega)$ satisfies the Helmholtz equation

$$\Delta u + k^2 u = 0, \quad \text{for } \mathbf{x}\in\mathbb{R}^2, \tag{1}$$

where $k=2\pi/\lambda$ is the wavenumber and $\lambda=2\pi c/\omega$ is the wavelength. For simplicity we drop the dependency on the frequency and write $u(\mathbf{x})\equiv u(\mathbf{x},\omega)$.

Remark 1. We assume that the frequency ω is not a resonant frequency of the scatterer we want to hide. Resonant frequencies are left for future studies.

Remark 2. Calling a cloak "active" can be ambiguous as one can refer to a cloak that can hide active sources [9] or a cloak that uses active sources to hide objects [11,12,19]. The cloaking method we present here is "active" in both senses as we use active devices to hide objects and in some simple situations it is possible to hide sources (see Remark 3). However here we focus only on cloaking scatterers.

2. Green's formula cloaks

We present the active interior cloak [19] and using an addition theorem for Hankel functions we show how this cloak can be replaced by a few multipolar sources (Section 2.2). The price to pay for using a finite number of sources is that the cloaked region and the region from which the object is invisible are smaller compared to the active interior cloak. We then make some geometric considerations (Section 2.3) to show that with the particular approach of Section 2.2 we need three or more sources to get a non-empty cloaked region.

2.1. Active interior cloak

Denote by D the region of $\mathbb{R}^2$ that we wish to cloak from a known incident field u_i. We also assume from now on that D is a simply connected bounded region of class C^2. The arguments in Section 2 can be easily generalized to the case where D is composed of several simply connected components. In order to cloak D, we construct a solution u_d to the Helmholtz Eq. (1) (in $\mathbb{R}^2$ excluding the boundary of D) such that

$$u_d(\mathbf{x}) = \begin{cases} -u_i(\mathbf{x}) & \text{for } \mathbf{x}\in D \\ 0 & \text{otherwise.} \end{cases} \tag{2}$$

Hence the total field u_d+u_i vanishes in D and is indistinguishable from u_i outside D. If a scatterer is placed inside D the scattered field u_s resulting from the incident field u_d+u_i is zero. Assuming u_i is an analytic solution to the Helmholtz Eq. (1) inside D, a field u_d satisfying Eq. (2) can be constructed using Green's formula (see e.g. [5])

$$u_d(\mathbf{x}) = \int_{\partial D} dS_{\mathbf{y}} \Big\{ -\Big(\mathbf{n}(\mathbf{y})\cdot\nabla_{\mathbf{y}} u_i(\mathbf{y})\Big) G(\mathbf{x},\mathbf{y}) + u_i(\mathbf{y})\mathbf{n}(\mathbf{y})\cdot\nabla_{\mathbf{y}} G(\mathbf{x},\mathbf{y}) \Big\}, \tag{3}$$

where $\mathbf{n}(\mathbf{y})$ is the unit outward normal to D at a point $\mathbf{y}$ on the boundary ∂D and the Green's function for the two dimensional wave equation is

$$G(\mathbf{x},\mathbf{y}) = \frac{i}{4} H_0^{(1)}(k|\mathbf{x}-\mathbf{y}|), \tag{4}$$

where $H_n^{(1)}$ is the n-th Hankel function of the first kind ([1], Section 9). The first term in the integrand in Eq. (3) can be interpreted as the potential due to a distribution of monopoles on the boundary ∂D (the single layer) while the second term can be interpreted as the potential due to a distribution of dipoles oriented normal to ∂D (the double layer).

In the frequency domain, the cloaking scheme we obtain is the same scheme proposed by Miller [19], where the single and double layer potentials in Eq.(3) are simulated with many sources completely surrounding the cloaked region D. We give an example of the field u_d generated by Green's formula (3) in Fig. 1. The effect of this active interior cloak can be seen in Fig. 2, where it is used to hide a kite shaped scatterer [4] with homogeneous Dirichlet boundary conditions. The field is virtually zero inside the cloaked region, so there are very little scattered waves to detect the object.

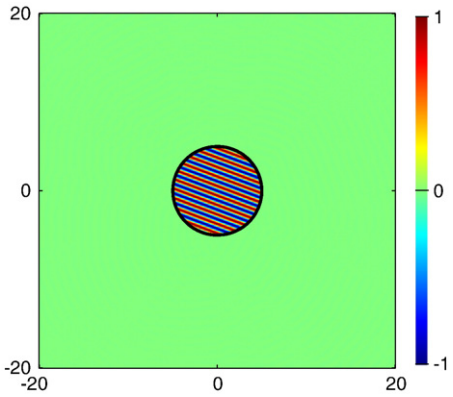

Fig. 1. The field u_d generated by Green's formula (3) The region D is the disk in thick lines with radius 5λ and the incident field is a plane wave with angle $5\pi/13$. The field u_d is very close to the incident field inside D and zero outside D. The integral in Eq. (3) is evaluated with the trapezoidal rule on 2^8 equally spaced points on ∂D. The axis units are in wavelengths λ.

2.2. Active exterior cloak

Our aim is to replace the single and double layer potentials on ∂D appearing in Eq. (3) by a few n_{dev} multipolar sources (what we call "cloaking devices") located at some points $\mathbf{x}_j \notin \partial D$. The advantage being that the cloaked region is no longer completely enclosed by a surface. The field generated by such sources can be written formally as

$$u_d^{(ext)}(\mathbf{x}) = \sum_{j=1}^{n_{dev}} \sum_{m=-\infty}^{\infty} b_{j,m} V_m\left(\mathbf{x}-\mathbf{x}_j\right), \tag{5}$$

where the coefficients $b_{j,m} \in \mathbb{C}$ are to be determined and

$$V_m(\mathbf{x}) \equiv H_m^{(1)}(k|\mathbf{x}|)\exp[im\arg(\mathbf{x})]$$

are radiating cylindrical waves. Here $arg(\mathbf{x})$ denotes the counterclockwise oriented angle from the vector $(1,0)$ to the vector $\mathbf{x}$. By a radiating solution to the Helmholtz equation, we mean it satisfies the Sommerfeld radiation condition (see e.g. [4]).

In [11,12] we presented a numerical scheme based on the singular value decomposition (SVD) to compute the coefficients $b_{j,m}$ in a way that $u_d^{(ext)}$ approximates u_d as defined in Eq. (2). We give next in Theorem 1 one way of obtaining these coefficients explicitly such that $u_d^{(ext)}(\mathbf{x}) = u_d(\mathbf{x})$ for $\mathbf{x}$ in a certain region $R \subset \mathbb{R}^2$, effectively reducing the cloaked region to $D \cap R$.

Let us assign to each source $\mathbf{x}_j$ a segment ∂D_j of the boundary. These segments are chosen such that they partition ∂D and $\partial D_i \cap \partial D_j$ is empty or a single point when $i \neq j$. An example of this setup is given in Fig. 3. The coefficients $b_{j,m}$ are given next.

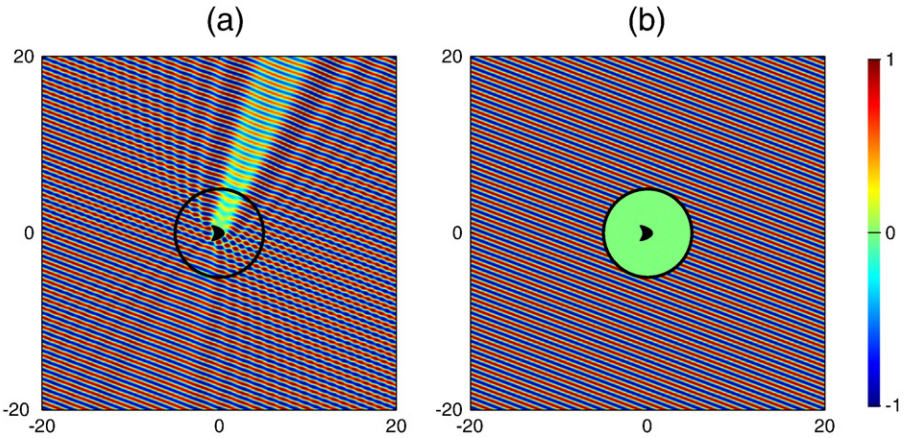

Fig. 2. Active interior cloak (a) inactive and (b) active. The region D where Green's formula is applied is the circle of radius 5λ in thick lines. The field inside the cloaked region D is virtually zero, so that outside the cloaked region the field is indistinguishable from the incident plane wave with direction $5\pi/13$. The axis units are in wavelengths λ.

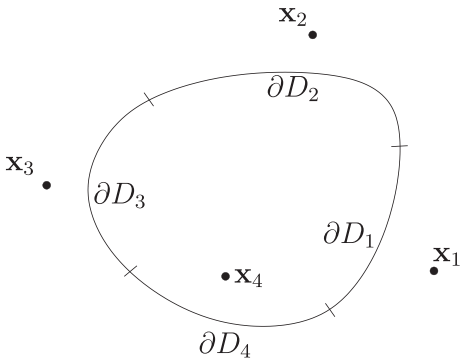

Fig. 3. Active exterior cloak construction. The contribution of portion ∂D_j to the single and double layer potentials in Green's formula (3) is replaced by a multipolar source located at $\mathbf{x}_j \notin \partial D$.

Theorem 1. *Multipolar sources located at $\mathbf{x}_j \notin \partial D$, $j = 1,\ldots,n_{dev}$, can be used to reproduce the active interior cloak in the region*

$$R = \bigcap_{j=1}^{n_{dev}} \left\{ \mathbf{x} \in \mathbb{R}^2 \,\middle|\, |\mathbf{x}-\mathbf{x}_j| > \sup_{\mathbf{y}\in\partial D_j} |\mathbf{y}-\mathbf{x}_j| \right\}.$$

The coefficients $b_{j,m}$ in Eq. (5) such that $u_d^{(ext)}(\mathbf{x}) = u_d(\mathbf{x})$ for $\mathbf{x} \in R$ are given by

$$b_{j,m} = \int_{\partial D_j} dS_{\mathbf{y}} \left\{ \left(-\mathbf{n}(\mathbf{y})\cdot\nabla_{\mathbf{y}} u_i(\mathbf{y})\right) \overline{U_m\left(\mathbf{y}-\mathbf{x}_j\right)} + u_i(\mathbf{y})\mathbf{n}(\mathbf{y})\cdot\nabla_{\mathbf{y}} \overline{U_m\left(\mathbf{y}-\mathbf{x}_j\right)} \right\} \tag{6}$$

for $j = 1,\ldots,n_{ext}$ and for $m \in \mathbb{Z}$. Here $U_m(\mathbf{x})$ are entire cylindrical waves,

$$U_m(\mathbf{x}) \equiv J_m(k|\mathbf{x}|)\exp[im\arg(\mathbf{x})].$$

Proof. Clearly, the integral over the whole boundary ∂D in Green's formula (3) can be written as the sum of the integrals over the segments ∂D_j. For segment ∂D_j, we use Graf's addition formula ([1], Section 9.1.79) to express the Green's function $G(\mathbf{x},\mathbf{y})$ as a superposition of multipolar sources located at $\mathbf{x}_j$,

$$\begin{aligned} G(\mathbf{x},\mathbf{y}) &= \frac{i}{4} H_0^{(1)}\left(k\left|\mathbf{x}-\mathbf{x}_j-\left(\mathbf{y}-\mathbf{x}_j\right)\right|\right) \\ &= \frac{i}{4} \sum_{m=-\infty}^{\infty} V_m\left(\mathbf{x}-\mathbf{x}_j\right)\overline{U_m\left(\mathbf{y}-\mathbf{x}_j\right)}, \end{aligned} \tag{7}$$

where the series converges absolutely and uniformly on compact subsets of $|\mathbf{x}-\mathbf{x}_j| > |\mathbf{y}-\mathbf{x}_j|$ (this can be seen by e.g. adapting Theorem 2.10 in [4] to two dimensions). Splitting the integral in Green's formula (5) into integrals over ∂D_j and using the expansion in Eq. (7) we get for $\mathbf{x} \in R$,

$$\begin{aligned} u_d^{(ext)}(\mathbf{x}) = \sum_{j=1}^{n_{dev}} \int_{\partial D_j} dS_{\mathbf{y}} \Bigg\{ &\left(-\mathbf{n}(\mathbf{y})\cdot\nabla_{\mathbf{y}} u_i(\mathbf{y})\right) \sum_{m=-\infty}^{\infty} V_m\left(\mathbf{x}-\mathbf{x}_j\right)\overline{U_m\left(\mathbf{y}-\mathbf{x}_j\right)} \\ &+ u_i(\mathbf{y})\mathbf{n}(\mathbf{y})\cdot\nabla_{\mathbf{y}} \sum_{m=-\infty}^{\infty} V_m\left(\mathbf{x}-\mathbf{x}_j\right)\overline{U_m\left(\mathbf{y}-\mathbf{x}_j\right)} \Bigg\} \end{aligned} \tag{8}$$

The desired Eq. (6) can be obtained by rearranging the infinite sum and the integral. For the first term in the integrals in Eq. (8), the uniform convergence of the series in Eq. (7) for $\mathbf{y} \in \partial D_j$ allows us to switch the infinite sum and the integral. The second term involves the gradient

$$\begin{aligned} \nabla_{\mathbf{y}} \overline{U_m\left(\mathbf{y}-\mathbf{x}_j\right)} = {} & k\frac{\mathbf{y}-\mathbf{x}_j}{|\mathbf{y}-\mathbf{x}_j|} J_m'\left(k|\mathbf{y}-\mathbf{x}_j|\right)\exp\left[-im\arg\left(\mathbf{y}-\mathbf{x}_j\right)\right] \\ & + J_m\left(k|\mathbf{y}-\mathbf{x}_j|\right)\left(-im\exp\left[-im\arg\left(\mathbf{y}-\mathbf{x}_j\right)\right]\right)\nabla_{\mathbf{y}}\arg\left(\mathbf{y}-\mathbf{x}_j\right). \end{aligned} \tag{9}$$

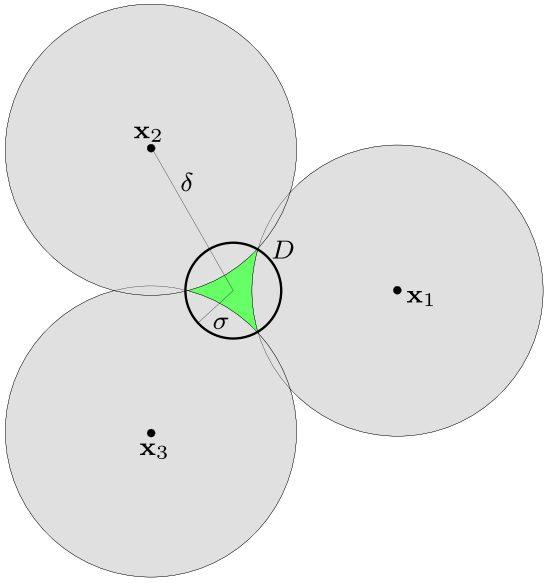

Fig. 4. A configuration for a cloak with three devices forming an equilateral triangle such that $|\mathbf{x}_j| = \delta$ for $j = 1,2,3$. The region D where we apply Green's formula is the disk of radius σ centered at the origin. The region $\mathbb{R}^2 \backslash R$ appears in gray. The green colored region is the effective cloaked region $D \cap R$.

Since we assumed $\mathbf{x}_j \notin \partial D$, the gradient

$$\nabla_{\mathbf{y}} \arg\left(\mathbf{y}-\mathbf{x}_j\right) = \frac{\left(\mathbf{y}-\mathbf{x}_j\right)^{\perp}}{|\mathbf{y}-\mathbf{x}_j|^2}, \quad \text{with } \mathbf{x}^{\perp} \equiv \begin{bmatrix} -x_2 \\ x_1 \end{bmatrix}, \tag{10}$$

is bounded for $\mathbf{y} \in \partial D_j$. Using the series representation for Bessel functions (see e.g. ([1], Section 9.3.1) and ([4], Section 3.4)) we can get the estimates

$$\begin{aligned} J_n(t) &= \frac{t^n}{2^n n!}(1 + \mathcal{O}(1/n)), & J_n'(t) &= \frac{t^{n-1}}{2^n (n-1)!}(1 + \mathcal{O}(1/n)) \\ H_n^{(1)}(t) &= \frac{2^n (n-1)!}{\pi i t^n}(1 + \mathcal{O}(1/n)) \end{aligned} \tag{11}$$

valid for $t > 0$ as $n \to \infty$, uniformly on compact subsets of $(0, \infty)$. Using Eq. (11) and the expression for the gradient in Eq. (9) we can estimate the terms

$$V_m\left(\mathbf{x}-\mathbf{x}_j\right) \nabla_{\mathbf{y}} \overline{U_m\left(\mathbf{y}-\mathbf{x}_j\right)} = \mathcal{O}\left(\frac{|\mathbf{y}-\mathbf{x}_j|^{m-1}}{|\mathbf{x}-\mathbf{x}_j|^m}\right) + \mathcal{O}\left(m \frac{|\mathbf{y}-\mathbf{x}_j|^m}{|\mathbf{x}-\mathbf{x}_j|^m}\right) \tag{12}$$

as $m \to \infty$ uniformly on compact subsets of $|\mathbf{x}-\mathbf{x}_j| > |\mathbf{y}-\mathbf{x}_j|$. Therefore the series in the second integrand of Eq. (8) converges absolutely and uniformly in ∂D_j and the infinite sum and the integral can be switched. □

Note that Theorem 1 does not guarantee that the effective cloaked region $D \cap R$ is not empty. However we do have that the device's field vanishes far away from the devices (i.e. $u_d^{(ext)}(\mathbf{x}) = 0$ for $|\mathbf{x}|$ large enough) because $\mathbb{R}^2 \backslash R$ is bounded. Later in Section 2.3 we give a specific configuration where $D \cap R$ is not empty.

Remark 3. In order to guarantee that the field $u_d(\mathbf{x})$ in Green's formula (3) vanishes outside D, we need an analytic incident field $u_i(\mathbf{x})$ inside D. If the field $u_i(\mathbf{x})$ is a radiating and also a C^2 solution to the Helmholtz Eq. (1) outside D (as it is the case when there are sources and non-resonant scatterers inside D), then Green's formula (3) converges outside D to $u_i(\mathbf{x})$ and inside D to zero (see e.g. [5]). This is the principle behind noise suppression [7] and the same idea could be used to cloak some (assumed known) active sources and scatterers in D.

Remark 4. Clearly the same Green's formula approach can be used to create illusions with active sources [27]: one can simultaneously cloak an object and generate waves that correspond to the scattering from a completely different object (the "virtual object"). All we need is knowledge of the scattered field $u_s^{virt}(\mathbf{x})$ generated by hitting the virtual object with the incident $u_i(\mathbf{x})$. Since $u_s^{virt}(\mathbf{x})$ is a radiating solution to the Helmholtz equation, to achieve illusion simply subtract u_s^{virt} from u_i in Eq. (6) (this is assuming that $u_s^{virt}(\mathbf{x})$ is C^2 outside D).

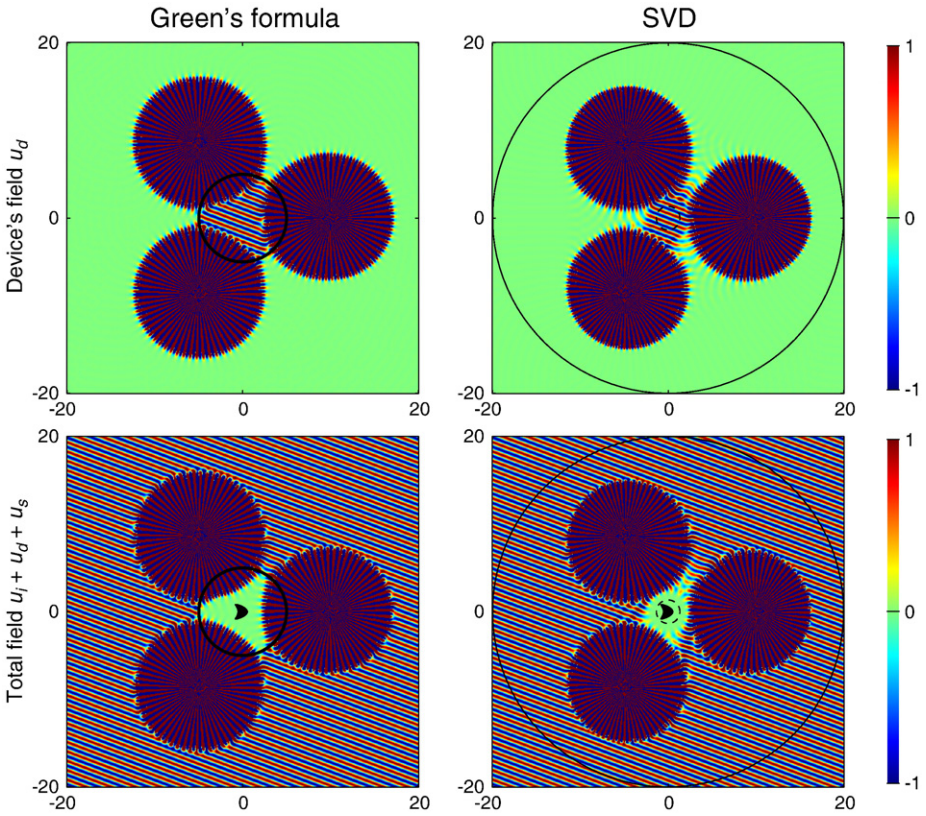

Fig. 5. Comparison of the Green's formula method (left column) and the SVD based method [11,12] (right column). The circle in thick lines is where we apply Green's formula. The dashed circle is where we enforce that the field be close to the incident field and the solid circle is where we enforce that the device's field is close to zero. The first row corresponds to the device's field and the second row to the total field.

Remark 5. The proof of Theorem 1 generalizes easily to the Helmholtz equation in three dimensions. We leave this generalization for future studies.

2.3. An explicit example of an active exterior cloak

In this Section we describe one possible realization of the cloak configuration presented in Theorem 1. First notice that with this particular method we need to have $n_{dev} \geq 3$ for a non-empty effective cloaked region $D \cap R$ (with D and R given as in Theorem 1). This is consistent with our numerical results in [11,12], as we observed that at least three devices are apparently needed to cloak plane waves with an arbitrary direction of propagation.

To see that at least three devices are needed, first notice that $\mathbb{R}^2 \backslash R = \cup_{j=1}^{n_{dev}} B_j$, where the B_j are disks centered at the j-th device location $\mathbf{x}_j$ and $\partial D_j \subset B_j$. We thus get

$$\partial D \subset \bigcup_{j=1}^{n_{dev}} B_j.$$

If we have only one device ($n_{dev} = 1$), then $D \subset \mathbb{R}^2 \backslash R$ and thus the effective cloaked region is empty. If we have two devices and D is simply connected, then we must also have $D \subset \mathbb{R}^2 \backslash R$, as the union of two non-disjoint disks is simply connected.

With three devices we take as an example the configuration shown in Fig. 4. Here the devices are located at a distance δ from the origin and are the vertices of an equilateral triangle. The region D where we apply Green's formula is the disk of radius σ centered at the origin. The circle ∂D is partitioned into three arcs ∂D_j, $j = 1,2,3$ of identical length which are chosen so that the distances $sup_{\mathbf{y} \in \partial D_j} |\mathbf{y} - \mathbf{x}_j|$ are equal for $j = 1,2,3$.

Simple geometric arguments show that the region R of Theorem 1 is the complement of the union of the three disks in gray in Fig. 4, with radius

$$r(\sigma, \delta) = \left((\sigma - \delta/2)^2 + 3\delta^2/4 \right)^{1/2}, \tag{13}$$

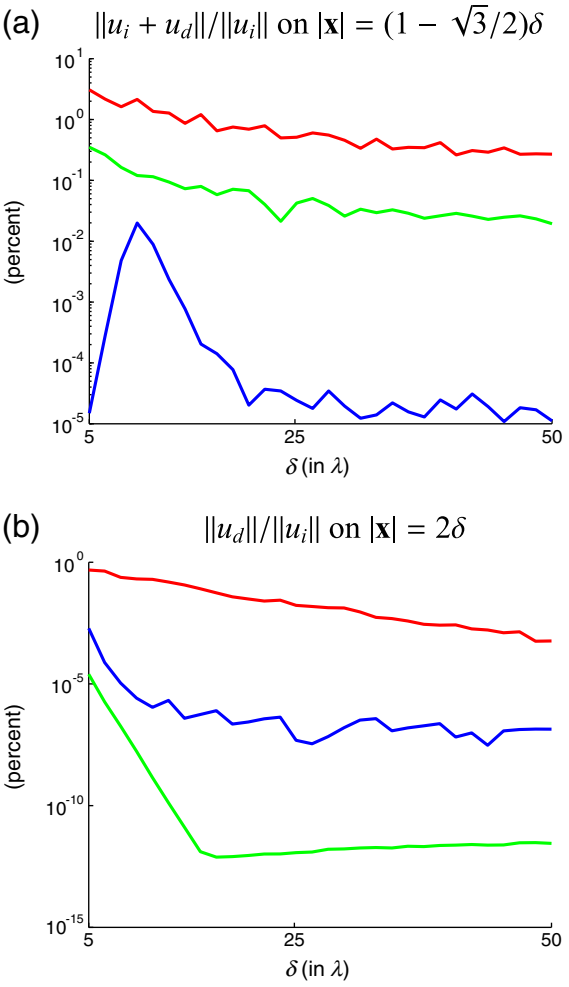

Fig. 6. Comparison of the cloak performance for the SVD method with $M(\delta)$ terms (blue) and the Green's identity method with $M(\delta)$ terms (red) and $2M(\delta)$ terms (green). In (a) we measure how small is the total field inside the cloaked region and in (b) how small is the device field far away from the devices.

and centered at $\mathbf{x}_j$, $j=1,2,3$. To get an idea of the dimensions of the effective cloaked region $R\cap D$ (in green in Fig. 4), we look at the radius of the largest disk that can be inscribed inside. This disk has radius

$$r_{eff}(\sigma,\delta) = \delta - r(\sigma,\delta). \tag{14}$$

Thus for fixed δ the largest effective cloaked region is obtained when $\sigma=\delta/2$, which corresponds to the case where the intersection of two of the disks in gray in Fig. 4 is a single point. Then the radius of the largest disk that can be inscribed inside $R\cap D$ is

$$r^*_{eff}(\delta) = \left(1-\sqrt{3}/2\right)\delta \approx 0.13\delta. \tag{15}$$

3. Numerical experiments

We compare the Green's formula based method with the geometry described in Section 2.3 and the maximal cloaked region size (i.e. $\sigma=\delta/2$) to an SVD based method [11,12]. In the SVD based method three distances are needed to describe the devices and the cloaked region: the distance δ from the devices to the origin, the radius α of the cloaked region and the radius γ of the circle

where we enforce that the device's field be small. The numerical experiments in [11,12] were done with $\alpha=\delta/5$ and $\gamma=2\delta$. To compare the cloaked regions for both methods we choose

$$\alpha = r^*_{eff}(\delta) = \left(1-\sqrt{3}/2\right)\delta$$

and leave γ unchanged. In this way the cloaked region for the SVD method should be the largest disk that fits inside the effective cloaked region $D\cap R$ of the Green's formula method.

We first compare in Fig. 5 the device's fields and the total field in the presence of a scatterer for both the SVD method and Green's formula method. Here the devices are at a distance $\delta=10\lambda$ from the origin, with $k=1$ and $\lambda=2\pi$. In all our numerical experiments the series in Eq. (5) is truncated to $m=-M,\ldots,M$. For the SVD method we follow the heuristic $M(\delta) = (k\delta/2)\left(1+\sqrt{3}/2\right)$ in [12], which for the setup of Fig. 5 gives $M(10\lambda)=59$. For comparison purposes we used the same number of terms in the Green's formula method. In both methods, the device's field cancels out the incident field in region near the origin without changing the incident plane wave. The region where the total field vanishes is larger for the Green's formula method than for the SVD method. And for the former method, the cloaked region seems larger than what is predicted by Section 2.3.

The fields near the devices (the "urchins" in Fig. 5) are very large as can be expected from the asymptotic behavior of Hankel functions at the origin

$$H_n^{(1)}(t) = \mathcal{O}\left(t^{-|n|}\right) \text{as } t\to 0 \text{ for } n\in\mathbb{Z}\setminus\{0\}.$$

The Green's formula allows us to replace each of the devices by a closed curve containing the device and with appropriate single and double layer potentials. The curves could be chosen as circles outside of which the device's field has reasonable values (e.g. less

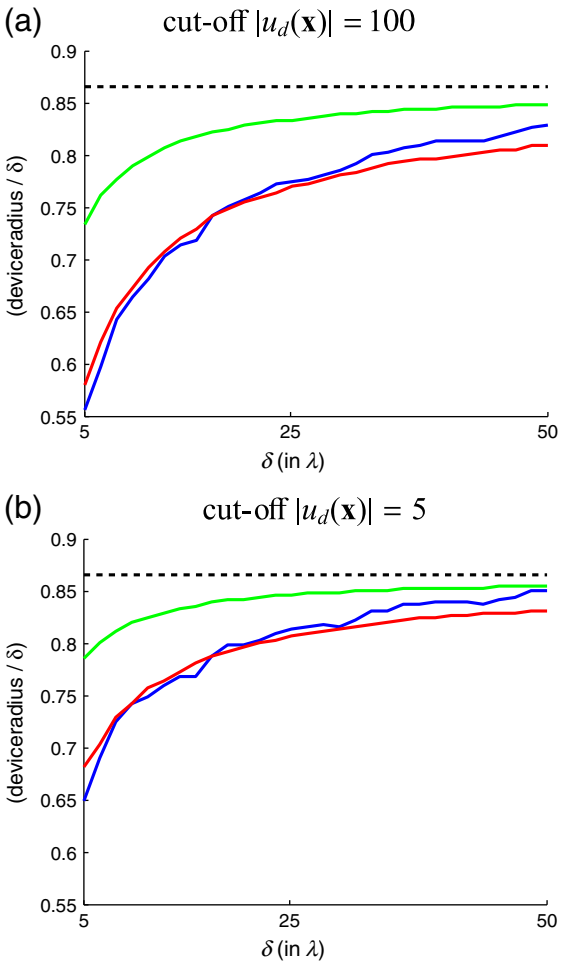

Fig. 7. Estimated device radius relative to δ for different values of δ. The dotted line corresponds to the radius of the devices if they were touching circles. The SVD method with $M(\delta)$ terms is in blue, the Green's identity method with $M(\delta)$ terms is in red and with $2M(\delta)$ terms in green.

than 5 or 100 times the magnitude of the incident field). For both methods these circles do not touch, leaving "throats" connecting the cloaked region to the exterior, so the cloaked region remains outside these "extended" devices.

We also considered larger cloaked regions in Fig. 6, keeping the same configuration as in Fig. 5 but taking $\delta \in [5,50]\lambda$. To evaluate the cloak performance we plot in Fig. 6 the quantity

$$\frac{||u_i + u_d||_{L^2}}{||u_i||_{L^2}}, \text{ on the circle } |\mathbf{x}| = \left(1-\sqrt{3}/2\right)\delta,$$

which measures how well the device's field cancels the incident field inside the cloaked region and

$$\frac{||u_d||_{L^2}}{||u_i||_{L^2}}, \text{ on the circle } |\mathbf{x}| = 2\delta,$$

which measures how small the device's field is relative to the incident field far away from the devices.[1] With the same number of terms $M(\delta)$ the SVD method outperforms the Green's formula method in both the cloaked region and far away from the devices. When $2M(\delta)$ terms are used for the Green's formula method, the relative errors improve, but the convergence of the series in Eq. (5) seems slower in the cloaked region than far away from the devices.

We estimate in Fig. 7 the size of the "extended" devices (i.e. the "urchins" where the device's field is large) by assuming they are disks centered at the device's locations $\mathbf{x}_i$. The disk radius for the device centered at $\mathbf{x}_i$ is estimated by finding the closest intersection of the level set $|u_d(\mathbf{x})| = \beta$ with each of the segments between $\mathbf{x}_i$ and the other two devices. The quantity plotted in Fig. 7 is the maximum of these distances rescaled by δ and is always below the radius at which the extended cloaking devices do not leave gaps with the exterior (for both cut-off values $\beta = 5$ and 10). The cost of having more terms in Green's formula is that the extended devices leave narrower throats. Presumably in the limit $M \to \infty$ these extended devices touch and correspond to the region $\mathbb{R}^2 \backslash R$ in Theorem 1.

Remark 6. A natural question is whether changing the integrals over ∂D_j in Eq. (6) to integrals over subsets of ∂D_j gives good cloaking devices. Since in the region R of Theorem 1 the device's field is identical to that of the active interior cloak, we can reformulate the question as follows: does making small openings in ∂D give a good active interior cloak? This is not the case because the resulting active interior cloak has fields identical in R to the fields for the cloak taking all of ∂D into account minus the fields obtained by integrating Green's formula (3) on the portions of ∂D that were excluded. The excluded portions have a monopole and dipole distributions that radiate and spoil the cloaking effect that we are after, even for small openings.

Acknowledgments

The authors are grateful for support from the National Science Foundation through grant DMS-070978. GMW and FGV wish to thank the Mathematical Sciences Research Institute, where this manuscript was completed.

References

[1] M. Abramowitz, I.A. Stegun, Handbook of Mathematical Functions, 9 edition, Dover, New York, NY, 1972.
[2] A. Alú, N. Engheta, Plasmonic and metamaterial cloaking: physical mechanisms and potentials, J. Opt. Pure Appl. Opt. 10 (2008) 093002.
[3] H. Chen, C.T. Chan, Acoustic cloaking and transformation acoustics, J. Phys. D Appl. Phys. 43 (11) (2010) 113001, doi:10.1088/0022-3727/43/11/113001.
[4] D. Colton, R. Kress, Inverse Acoustic and Electromagnetic Scattering Theory, Volume 93 of Applied Mathematical Sciences, second edition, Springer-Verlag, Berlin3-540-62838-X, 1998.
[5] D. L. Colton and R. Kress. *Integral equation methods in scattering theory*. Pure and Applied Mathematics (New York). John Wiley & Sons Inc., New York, 1983. ISBN 0-471-86420-X. A Wiley-Interscience Publication.
[6] M. Farhat, S. Guenneau, S. Enoch, A.B. Movchan, Cloaking bending waves propagating in thin elastic plates, Phys. Rev. B 79 (2009) 033102.
[7] J.E. Ffowcs Williams, Review lecture: anti-sound, Proc. R. Soc. A 395 (1984) 63–88.
[8] A. Greenleaf, M. Lassas, G. Uhlmann, Anisotropic conductivities that cannot be detected by EIT, Physiol. Meas. 24 (2003) 413–419.
[9] A. Greenleaf, Y. Kurylev, M. Lassas, G. Uhlmann, Full-wave invisibility of active devices at all frequencies, Commun. Math. Phys. 275 (2007) 749–789 ISSN 0010-3616.
[10] A. Greenleaf, Y. Kurylev, M. Lassas, G. Uhlmann, Cloaking devices, electromagnetic wormholes, and transformation optics, SIAM Rev. 51 (1) (2009) 3–33.
[11] F. Guevara Vasquez, G.W. Milton, D. Onofrei, Active exterior cloaking for the 2D Laplace and Helmholtz equations, Phys. Rev. Lett. 103 (2009) 073901.
[12] F. Guevara Vasquez, G.W. Milton, D. Onofrei, Broadband exterior cloaking, Opt. Express 17 (2009) 14800–14805, doi:10.1364/OE.17.014800.
[13] M.J.M. Jessel, G.A. Mangiante, Active sound absorbers in an air duct, J. Sound Vib. 23 (3) (1972) 383–390.
[14] Y. Lai, H. Chen, Z.-Q. Zhang, C.T. Chan, Complementary media invisibility cloak that cloaks objects at a distance outside the cloaking shell, Phys. Rev. Lett. 102 (2009) 093901.
[15] Y. Lai, J. Ng, H. Chen, D. Han, J. Xiao, Z.-Q. Zhang, C.T. Chan, Illusion optics: the optical transformation of an object into another object, Phys. Rev. Lett. 102 (25) (Jun 2009) 253902, doi:10.1103/PhysRevLett.102.253902.
[16] U. Leonhardt, Optical conformal mapping, Science 312 (2006) 1777–1780.
[17] U. Leonhardt, T. Tyc, Broadband invisibility by non-Euclidean cloaking, Science 323 (2009) 110–112.
[18] G.D. Malyuzhinets, One theorem for analytic functions and its generalizations for wave potentials, Third All-Union Symposium on Wave Diffraction, (Tbilisi, 24–30 September 1964), Abstracts of Reports, 1964.
[19] D.A.B. Miller, On perfect cloaking, Opt. Express 14 (2006) 12457–12466.

[1] The values of $\|u_d\|/\|u_i\|$ reported in Fig. 4b in [12] are, due to a normalization mistake, up to a factor of $\sqrt{10}$ smaller than what they should be. In the logarithmic scale we use to display this quantity, the resulting shift is small and our conclusions remain the same.

[20] G.W. Milton, N.-A.P. Nicorovici, On the cloaking effects associated with anomalous localized resonance, Proc. R. Soc. Lond. A Math. Phys. Sci. 462 (2006) 3027–3059 ISSN 0080-4630.
[21] G.W. Milton, N.-A.P. Nicorovici, R.C. McPhedran, K. Cherednichenko, Z. Jacob, Solutions in folded geometries, and associated cloaking due to anomalous resonance, New J. Phys. 10 (2008) 115021.
[22] N.-A.P. Nicorovici, G.W. Milton, R.C. McPhedran, L.C. Botten, Quasistatic cloaking of two-dimensional polarizable discrete systems by anomalous resonance, Opt. Express 15 (2007) 6314–6323.
[23] J.B. Pendry, D. Schurig, D.R. Smith, Controlling electromagnetic fields, Science 312 (2006) 1780–1782.
[24] A.W. Peterson, S.V. Tsynkov, Active control of sound for composite regions, SIAM J. Appl. Math. 67 (2007) 1582–1609.
[25] M.G. Silveirinha, A. Alù, N. Engheta, Cloaking mechanism with antiphase plasmonic satellites, Phys. Rev. B 78 (20) (Nov 2008) 205109, doi:10.1103/PhysRevB.78.205109.
[26] I.I. Smolyaninov, V.N. Smolyaninova, A.V. Kildishev, V.M. Shalaev, Anisotropic metamaterials emulated by tapered waveguides: application to optical cloaking, Phys. Rev. Lett. 102 (2009) 213901.
[27] H.H. Zheng, J.J. Xiao, Y. Lai, C.T. Chan, Exterior optical cloaking and illusions by using active sources: a boundary element perspective, Phys. Rev. B 81 (19) (May 2010) 195116, doi:10.1103/PhysRevB.81.195116.